# Laser-induced free-carrier and temperature gratings in silicon

H. J. Eichler, F. Massmann, E. Biselli, K. Richter, M. Glotz, L. Konetzke, and X. Yang*
*Optisches Institut, Technische Universität, 1000 Berlin 12, Germany*
(Received 8 September 1986; revised manuscript received 9 March 1987)

Dynamic gratings have been produced in silicon excited with nano- and picosecond pulses at 1.06 $\mu$m wavelength and then probed at 1.06 and 1.3 $\mu$m. The diffraction efficiency is given by a Bessel function of the refractive-index change. The resulting modulation of the diffracted light experimentally proves that the phase-grating contribution is dominant. Free-carrier and thermal refractive-index changes are separated due to their different time dependences and opposite signs. The dispersion volume $n_{e\text{-}h} = 1.4 \times 10^{-21}$ cm$^3$ of the electron-hole pairs at 1.3 $\mu$m was measured. The time dependence of the diffraction efficiency is described by diffusion and recombination of the electron-hole pairs and by heat conduction.

## I. INTRODUCTION

Silicon is a highly effective material for real-time holography,[1-4] phase conjugation by four-wave mixing,[5-8] and laser pulse amplification by coherent two-wave mixing.[9,10] Its combination with neodymium lasers emitting at 1.06 $\mu$m is particularly useful because the laser photon energy matches the silicon band gap resulting in an absorption coefficient of 10 cm$^{-1}$ at room temperature. This allows one to use comparatively thick samples, which is important for high-power applications to avoid sample heating. In addition, the material absorption can be adjusted to the sample thickness over orders of magnitude by temperature tuning.[11,12]

The wave-interaction processes are due to dynamic refractive-index gratings resulting from laser-induced electron-hole pairs and temperature changes. Since the grating decay times range from picoseconds to nanoseconds, the highest wave-mixing efficiencies are obtained with pulsed lasers.

Laser-induced dynamic gratings in silicon have been studied extensively to understand and optimize wave-mixing applications and also to determine material properties such as carrier decay and diffusion times.[13-23] The aim of the present paper is to investigate the grating mechanisms at high excitation energy densities up to 300 mJ/cm$^2$, which is near the damage threshold of the material surface. The highest two- and four-wave mixing densities are observed at such fluences[5,6] and therefore it seems important to investigate the grating properties in this regime. In addition, silicon is a well-characterized material and investigations of high-excitation laser-induced grating effects provide a conceptual basis also for studies of other materials.

## II. EXPERIMENTAL ARRANGEMENT

The experimental setup (Fig. 1) is similar to that in a preceding paper.[15] Two intersecting Nd:YAG (where YAG is yttrium aluminum garnet) laser beams at 1.06 $\mu$m produced the gratings. The transverse mode control was improved so that intensity fluctuations across the beam cross section were reduced. The dynamic gratings were probed with quasi-cw lasers at 1.06 $\mu$m as previously[15] and in addition at 1.3 $\mu$m. This wavelength is well below the band gap so that absorption is negligible. Therefore, the 1.3-$\mu$m probe beam does not change the free-carrier density, which is particularly important if the excitation energy and resulting carrier density are small.

A $Q$-switched Nd:YAG laser[15] with 10–20 ns pulse width was used for grating excitation. The laser energy was varied with a single-stage Nd:YAG amplifier and neutral-density filters. A beam splitter produced two pulses with equal power intersecting in the sample. The grating spacing $\Lambda = 5-100$ $\mu$m is determined by the intersection angle. The fundamental-mode beam diameter on the silicon sample amounted to 3 mm. An aperture with about 1 mm diameter was used to select the central part of the beam resulting in an energy density which was spatially constant to about 10%. The excitation energies given in Figs. 2 and 7 are measured behind the aperture. The laser-induced dynamic grating was probed with a spiking Nd:YAG laser at 1.3 $\mu$m with prism wavelength tuning. The first spike with a duration of 1 $\mu$s was used so that only the initial time regime of the gratings could be probed where electronic effects dominate (Fig. 2).

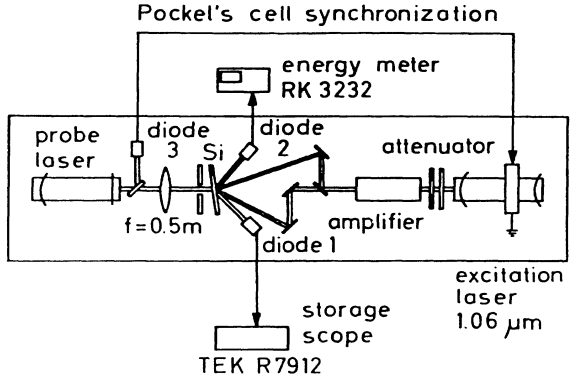


FIG. 1. Apparatus for production of laser-induced gratings and time-resolved measurement of the diffraction efficiency.

 

Measurements were done also with a quasi-cw probe laser with a wavelength of 1.06 $\mu$m. This laser emitted a constant output power for about 100 $\mu$s and was used to investigate the comparatively slow thermal grating decay (Sec. VI). In addition, picosecond pump and probe experiments were performed to measure the fast decay of free-carrier gratings at small grating periods (Fig. 6). A passively mode-locked Nd:YAG laser was used with an electro-optic selector producing single pulses with 30 ps full width at half maximum and 2 mJ energy after amplification.

The silicon samples had a (111) orientation and were weakly phosphorus doped resulting in a specific resistance of 100 $\Omega$ cm. The total effective reflectivity of the polished samples amounted to $R_{\text{eff}}=32\%$. Samples with $d=330$, 500, and 560 $\mu$m thickness were used.

## III. FREE-CARRIER GRATINGS AND TIME-DEPENDENT DIFFRACTION

The time dependence of the diffracted intensity changed significantly with the excitation energy as shown in Fig. 2. At low incident energy $W=0.05$ mJ, the diffracted power increases monotonically during the excitation pulse, which had a width of about 20 ns at half maximum. The rise time of the diffracted power amounts to about 40 ns and is explained by integrating the pulse shape. At higher incident energies $W>0.1$ mJ, the diffracted power or intensity $I_1$ exhibits strong oscillations which are explained by the Bessel-function dependence[15,21] of the grating efficiency on the refractive-index amplitude $\Delta n$:

$$I_1=ITJ_1^2(2\pi\Delta nd/\lambda) . \tag{1}$$

Here $I$ is the incident intensity, $T$ the sample transmission, $\lambda$ the probe wavelength, $d$ the sample thickness, and $J_1$ the first-order Bessel function.

The refractive-index modulation is due to excitation of electron-hole pairs with density ($\Delta n_N$) and a temperature change due to electron-hole recombination and free-carrier absorption ($\Delta n_T$)

$$\Delta n=\Delta n_N+\Delta n_T . \tag{2}$$

At low excitation as in Fig. 2 ($W<0.3$ mJ) the thermal change of the refractive index is negligible and the electronic change is given by[15]

$$n_N=n_{e\text{-}h}N'(t)$$
$$=\frac{n_{e\text{-}h}}{dh\nu}\int_{-\infty}^{t} I_a(t')\exp[-(t-t')/\tau]dt' . \tag{3}$$

Here $N'(t)$ is the spatial amplitude of the refractive-index modulation, $n_{e\text{-}h}$ the "dispersion volume," i.e., the refractive-index change due to one electron-hole pair per unit volume, $d$ the sample thickness, $h\nu$ the photon energy of the excitation laser, $I_a(t)$ the absorbed intensity, and $\tau$ the grating decay time. Figure 3 shows schematically

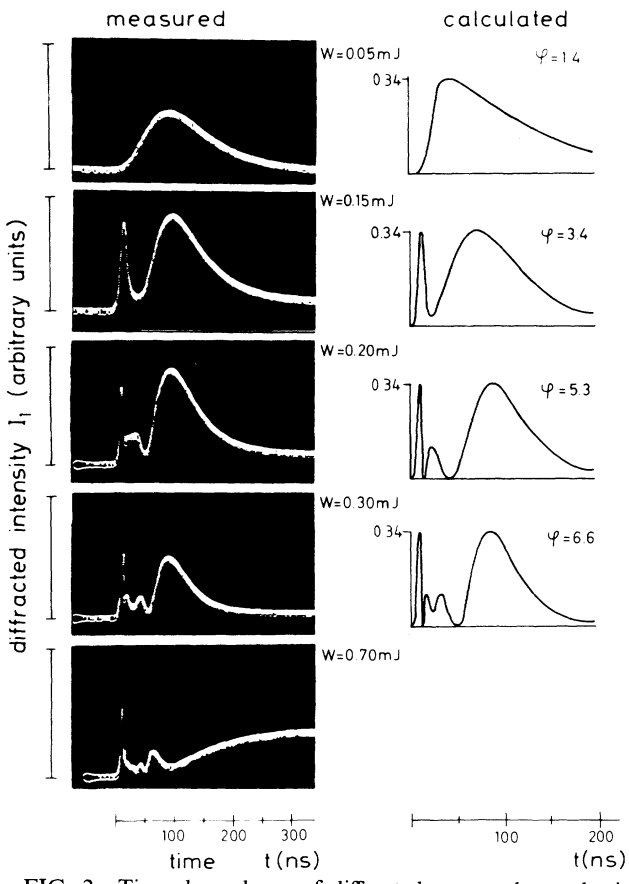


FIG. 2. Time dependence of diffracted power observed with diode 1 in Fig. 1. Excitation laser wavelength, 1.06 $\mu$m; $\tau_p=20$ ns pulse width. Probe laser wavelength, 1.3 $\mu$m; 1 $\mu$s pulse width. $W$ is the excitation energy in aperture area measured with diode 2 adjusted to detect reflected excitation beams. $\varphi$ is the phase grating amplitude chosen to match the calculated to the measured curves.

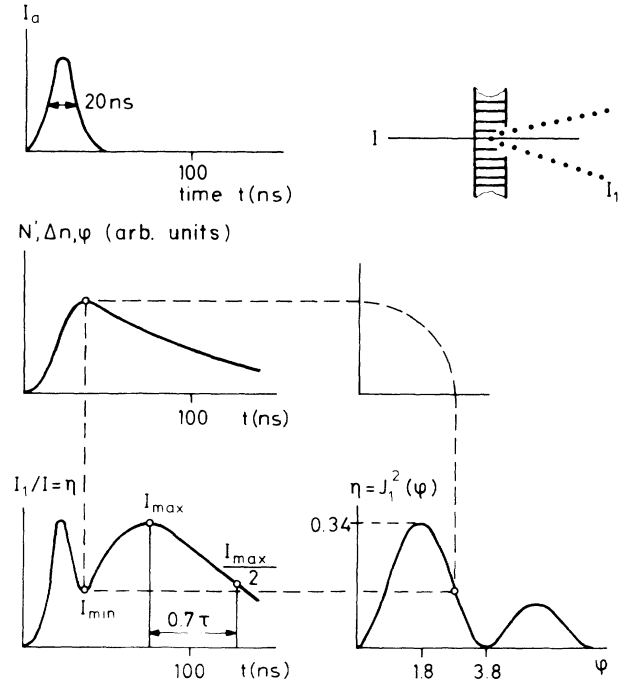


FIG. 3. Short excitation pulse $I_a$ produces free-carrier grating with amplitude $N'$ and refractive index change $\Delta n$. Oscillations in the time-dependent diffraction efficiency $\eta$ are due to Bessel-function dependence $J_1^2(\varphi)$ on phase amplitude $\varphi$.

that a short excitation pulse $I_a(t)$ produces a sharply rising and slowly decaying $e$-$h$ density and corresponding refractive-index change which results in a modulated diffraction efficiency $\eta$. Calculated time dependences of the diffracted power for different maximum refractive index changes are given in Fig. 2. An excitation pulse $I_a(t)$ with a Gaussian time shape was used for the calculations. $I_a(t)$ is the total intensity of both excitation beams. The average intensity is equal to the spatial amplitude of the intensity because both beams have the same power.

The grating decay times have been chosen to match the calculated to the experimental curves. A detailed evaluation of grating decay times will be described later. Comparing the experimental and calculated time dependence of the diffracted intensity, it can be noted that, while the theoretical diffracted intensity goes to zero, the minimum measured diffraction signal is always greater than approximately 20% of the peak signal. This is explained by considering the limited time resolution of the photodiode and digitizer filling up the experimental intensity minimum. Spatial energy density fluctuations of the excitation beams have the same effect. These fluctuations lead to an uncertainty of the carrier density as will be discussed later.

The agreement between the measured and calculated time dependences of the diffracted power proves for the first time that the Bessel-function approximation Eq. (1) is valid for the diffraction efficiency of a thin laser-induced phase grating. This approximation has been derived first by Raman and Nath[24] for diffraction of light at ultrasonic waves. We used Eq. (1) already in a preceding paper[15] but a good agreement between experiments and calculations is obtained only now.

The highest excitation energy $W=0.7$ mJ in Fig. 2 results in a time dependence which cannot be explained by Eqs. (1)–(3). The second strong maximum is much smaller in comparison to $W \leq 0.3$ mJ. The reduction of this maximum is due to free-carrier absorption.

In addition, a third broad maximum develops with a large delay of about 300 ns after the excitation pulse. This maximum is due to a thermal refractive index change. Thermal effects are discussed in Sec. VI.

## IV. DISPERSION VOLUME $n_{e\text{-}h}$

According to Eq. (3) the refractive-index change $\Delta n_N$ is linearly dependent on the carrier density $N'$. The quantity $n_{e\text{-}h}$ is called "dispersion volume" because it has the dimension $m^3$ and relates the carrier density to the refractive index. Similarly, the free-carrier absorption coefficient is described by a "cross section" $\sigma_{e\text{-}h}$.

The linear dependence of $\Delta n_N$ on $N'$ has been checked by calculating the total number of carriers $N_t'$ produced by absorption of a short pulse with energy density $E'$ from

$$N_t' = \frac{2}{d\sigma} \ln \left[ 1 + \frac{\sigma}{2} \frac{E'}{h\nu} \frac{(1-R)(1-T_0)}{1-RT_0} \right] . \tag{4}$$

This equation has been derived by averaging the carrier density given in[25] over the sample thickness. Equation (4) takes into account that only a fraction of the absorbed photons produces free carriers; the other fraction is absorbed by the generated carriers leading to lattice heating. $R$ is the reflectivity of the sample surface and $T_0$ the net transmission at low intensity. In deriving Eq. (4) only one reflection of the incident beams has been considered and the intensity dependence of the transmission has been neglected.

If $E'$ is sufficiently small, Eq. (4) is approximated by

$$N_t' \approx \frac{E'(1-R)(1-T_0)}{dh\nu(1-RT_0)} = \frac{E'(1-R_{\text{eff}}-T_{\text{eff}})}{dh\nu} = \frac{E_a}{dh\nu} . \tag{5}$$

Here $R_{\text{eff}}$ and $T_{\text{eff}}$ give the total reflection and transmission of the sample, which can be measured experimentally, and $E_a$ is the absorbed energy density. The carrier density calculated from Eq. (5) is only 20% larger than that of Eq. (4) at an energy density $E'=100$ mJ/cm$^2$. Because other uncertainties in the determination of the carrier density are larger, Eq. (5) is a reasonable approximation.

The corresponding refractive index change is derived from the experimental diffraction efficiency as shown in Fig. 2. Starting from Eq. (1) the maximum refractive index change is obtained from the ratio of the minimum diffracted intensity to the maximum by

$$J_1^2(2\pi\Delta n_t/\lambda) = 0.34 I_{\max}/I_{\min} . \tag{6}$$

This method is very convenient since it is not necessary to make an absolute measurement of the diffraction efficiency.

The measured refractive index change versus carrier density is shown in Fig. 4. A linear dependence is obtained up to a carrier density of $1.5\times10^{18}$ cm$^{-3}$. The slope gives a dispersion volume of $n_{e\text{-}h}=1.4\times10^{-21}$ cm$^3$. For large values of the carrier density ($N_t' \geq 2\times10^{18}$

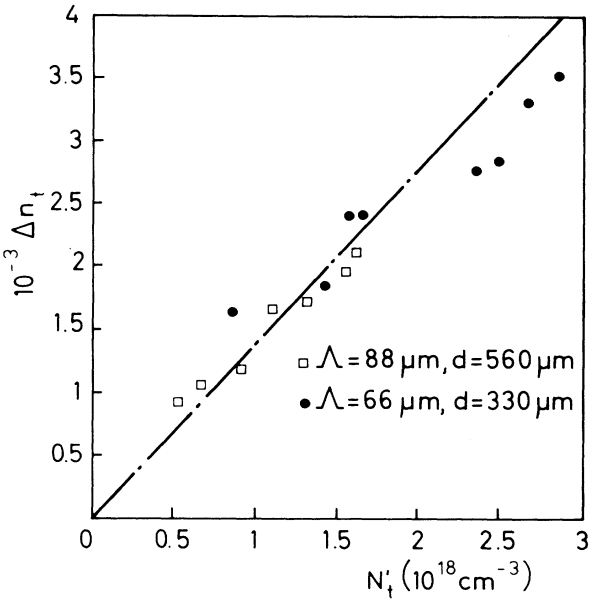


FIG. 4. Refractive index change $\Delta n_t$ vs carrier density $N_t'$ derived from measurements as shown in Fig. 2.

$cm^{-3}$), the refractive index increases sublinearly with the carrier density calculated from Eq. (5). This is due to free-carrier absorption as explained above.

The experimental value for $n_{e\text{-}h}$ agrees with the known effective optical mass of an electron-hole pair, $m^* = 0.17 m_0$, using[21,26,27]

$$n_{e\text{-}h} = \frac{-e^2}{2 n_0 m^* \epsilon_0 \omega^2} . \tag{7}$$

Note that the refractive index change is measured here at 1.3 $\mu$m and not at 1.06 $\mu$m as in previous experiments.[1-15]

## V. FREE-CARRIER GRATING DECAY TIMES

The decay of the free-carrier grating with carrier density $N(x,t)$ is described by

$$\frac{\partial N}{\partial t} + CN^3 - D\frac{\partial^2 N}{\partial x^2} = 0 . \tag{8}$$

Here $C$ is the Auger-recombination coefficient and $D$ the ambipolar diffusion constant. Due to interference of the pump beams, the carrier density is spatially modulated:

$$N(x,t) = N'(t)\cos(2\pi x/\Lambda) + N''(t) . \tag{9}$$

Equation (9) gives the first terms of a Fourier expansion of $N(x,t)$. Higher spatial harmonics are possible but are not of interest here since only first-order diffraction is observed experimentally. Combination of Eqs. (8) and (9) results in the following equation for the grating amplitude $N'(t)$:

$$\frac{dN'(t)}{dt} + 3C(N'')^2 N'(t) + D\frac{4\pi^2}{\Lambda^2} N'(t) = 0 . \tag{10}$$

The decay of the amplitude $N'(t)$ is given by Auger recombination and diffusion. The decay of the average carrier density $N''(t)$ is given by Auger recombination only and is much slower than the decay of $N'(t)$. Therefore $N''(t)$ may be considered as a constant parameter $N_0$ in Eq. (10) and an exponential decay of $N'(t)$ is obtained:

$$N = N_0 \exp(-t/\tau) , \tag{11}$$

with

$$\frac{1}{\tau} = \frac{4\pi^2 D}{\Lambda^2} + 3CN_0^2 . \tag{12}$$

Experimental values for $\tau$ are derived from the time dependence of the diffracted intensity. Combination of Eqs. (1) and (11) gives the result that the half-minimum period (Fig. 4) of the diffracted intensity corresponds to $0.7\tau$.

Numerical values of the free-carrier grating decay time are given in Fig. 5 in dependence of the initial carrier density $N_0$. Using Eq. (12) a diffusion coefficient $D = 7 \pm 3$ $cm^2/s$ and Auger coefficient $C = (4 \pm 3) \times 10^{-31}$ $cm^6/s$ is obtained. The large errors given for $D$ and $C$ are caused by errors of the experimental grating decay $\tau$ and carrier density. The measurement of the grating decay time is done with a pulsed probe laser with fluctuating pulse shape and position. This leads to an error of about $\pm 10\%$ for $\tau$. The carrier density is calculated from the exciting-laser-pulse energy and the absorption coefficient of silicon for which an uncertainty of $\pm 10\%$ is estimated. The exciting beam profile is not rectangular but varies over the beam cross section for about 10%. In total, an error of $\pm 30\%$ is estimated for the carrier density $N_0$. Because the Auger coefficient $C$ depends quadratically on $N_0$ and linearly on $\tau$ an error of 70% results for $C$.

It is assumed in the evaluation of Fig. 5 that the diffusion coefficient is independent of the carrier density, which has not been proved. In addition, the experimental decay time defined in Fig. 3 is affected also by thermal refractive index changes as outlined in Sec. VI. Therefore $D$ and $C$ should be considered as fit parameters which could deviate from the ambipolar diffusion coefficient and Auger coefficient determined by other methods.

A comparison of the coefficient $C$ with results of Dziewior and Schmid[28] and Svantesson and Nilsson[29] gives good agreement ($3.8 \times 10^{-31}$ and $3.4 \times 10^{-31}$ $cm^6/s$). Recent measurements of Grimaldi *et al.*[30] give a larger Auger coefficient ($10^{-30}$ $cm^6/s$).

The constant $D$ is smaller than measured by us[15] previously ($11 \pm 3$ $cm^2/s$). Because we use a 1.3-$\mu$m Nd:YAG laser as a probing light source, no additional carriers are produced by the probe radiation. In our previous experiment[15] a 1.06-$\mu$m probe laser was used, which reduced the measured grating decay time by carrier production. A smaller grating decay time was explained by stronger diffusion. Further, we reduced the energy fluctuations of the exciting beam using a mode selector in our oscillator and an aperture in front of our sample to get a nearly rectangular energy profile (see also above). Because the apparatus was improved in these ways, the new result seems more reliable. The error of $\pm 3$ $cm^2/s$ in our previous paper was obtained by statistical averaging and was not based on a consideration of the various systematic errors

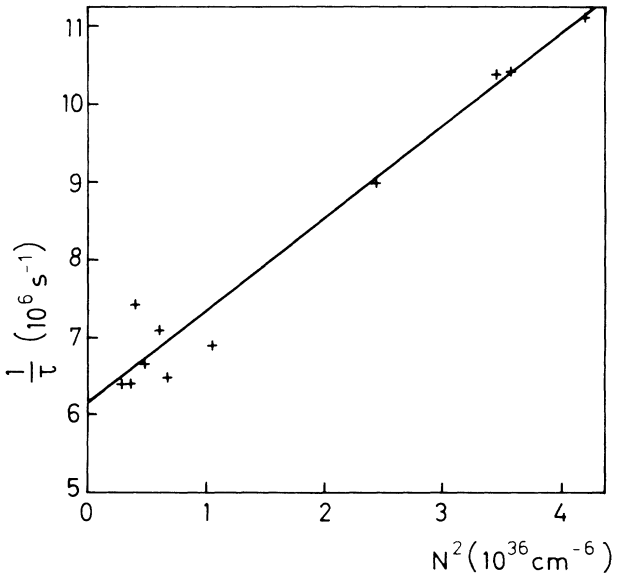


FIG. 5. Grating decay time $\tau$ vs carrier density derived from measurements as shown in Fig. 2. Grating period $\Lambda = 66$ $\mu$m.

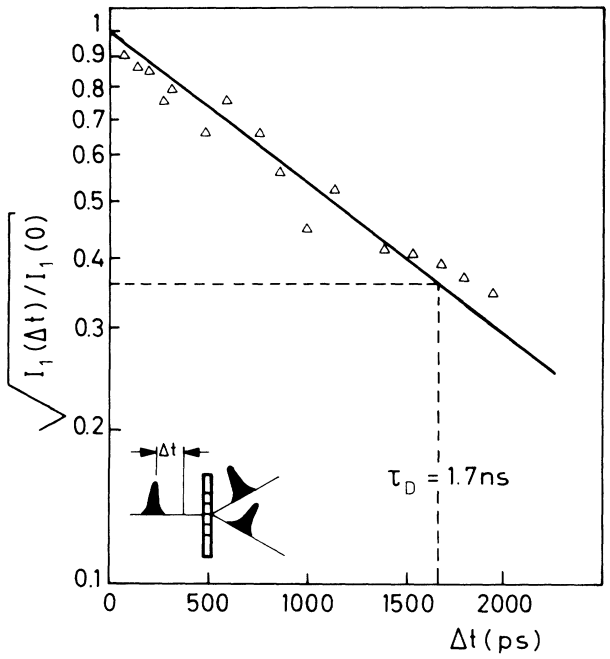


FIG. 6. Picosecond pump and probe experiment to measure grating decay for small grating period $\Lambda = 6.8$ $\mu$m.

discussed above.

An additional measurement was performed with a picosecond laser (Fig. 6). This experiment resulted in a decay of $\tau = 1.7$ ns at a grating period of 6.8 $\mu$m. Since the excitation energy and carrier density were small, a diffusion coefficient of $D = 7$ cm$^2$/s can be directly calculated from $\tau$. This value agrees with the other measurements. Picosecond experiments at higher excitation and other grating periods indicated lifetime shortening similarly as shown in Fig. 5.

The measured constant $D$ is smaller than the low-density ambipolar diffusion constant $D^0 = 18$ cm$^2$/s. However, calculations[31] taking into account self-energy shifts of the free-carrier band edges predict a decrease of the diffusion constant for carrier densities of $10^{17}$–$10^{19}$ cm$^{-3}$ down to 15 cm$^2$/s. This value is still larger than our experimental observations but agrees with Ref. 16. A decrease of the diffusion coefficient $D$ at carrier densities of $10^{18}$–$10^{19}$ cm$^{-3}$ is indicated also in Ref. 32 using a different experimental technique.

## VI. THERMAL GRATINGS

Figure 7 shows the time dependence of the diffracted light on a larger scale. These measurements have been performed with a quasi-cw probe laser at 1.06 $\mu$m. The noise of the curves in Fig. 7 is due to relaxation oscillations of the probe laser.

The time dependence of the diffracted light exhibits two sharp maxima which are predominantly due to the free-carrier grating (compare Fig. 2) and correspond to the first maximum of the Bessel function [Eq. (1)] which is passed twice during the buildup and decay of the carrier

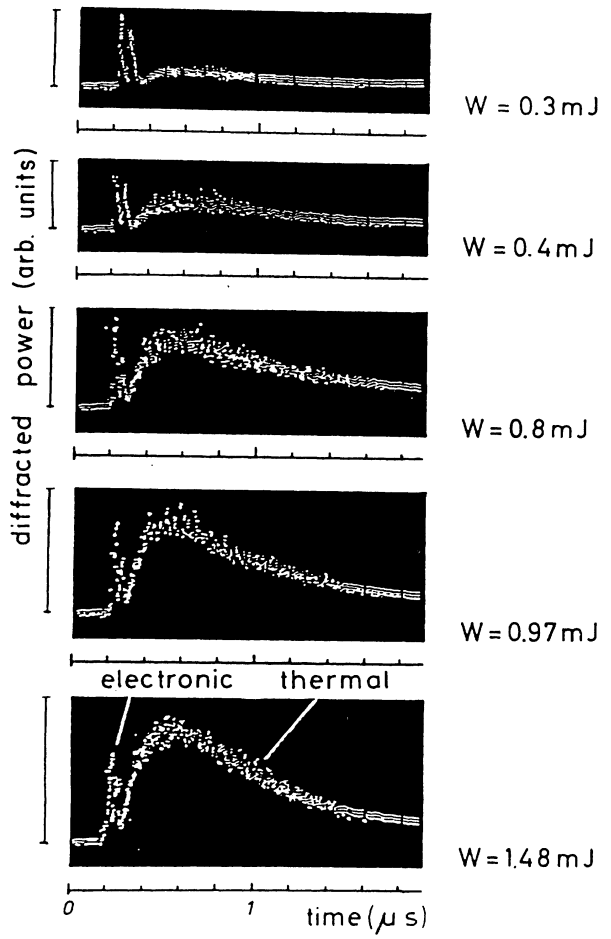


FIG. 7. Time dependence of diffracted power observed with the apparatus in Fig. 2 using a probe laser with a 100-$\mu$s pulse and 1.06-$\mu$m wavelength.

density. In Fig. 7 a third broad maximum occurs with a delay of about 200–300 ns after the two initial spikes. The value of this maximum increases with the excitation energy. This broad maximum is explained by an additional temperature grating with a refractive-index amplitude

$$\Delta n_T = \frac{\partial n}{\partial T} T(x,t) \ . \tag{13}$$

The temperature distribution $T(x,t)$ in the silicon sample is described by

$$\frac{\partial T(x,t)}{\partial t} - D_T \frac{\partial^2 T(x,t)}{\partial x^2} = \frac{N(x,t)}{\rho_0 c} [h\nu C N^2 + \sigma_{e\text{-}h} I(x,t)] \ . \tag{14}$$

Here $D_T$ is the temperature diffusivity, $\rho_0$ the density, and $c$ the specific heat of the sample. The term $CN^3 h\nu/\rho_0 c$ describes sample heating due to carrier recombination, and $\sigma_{e\text{-}h} NI/\rho_0 c$ corresponds to free-carrier absorption. A numerical estimate shows that free-carrier absorption is the dominant mechanism leading to sample heating.

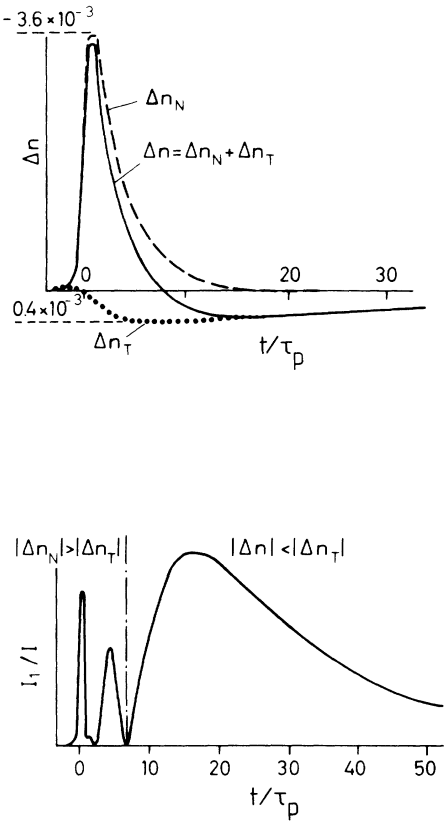


FIG. 8. Calculated time dependence of electronic $\Delta n_N$, thermal $\Delta n_T$, and total $\Delta n$ refractive-index change and diffraction efficiency $I_1/I$ for a combined free-carrier and temperature grating at 200 mJ/cm$^2$ excitation energy density.

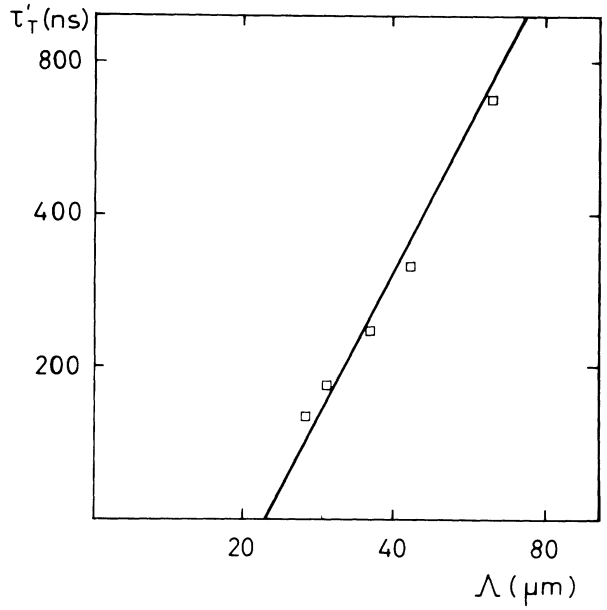


FIG. 9. Temperature grating decay time $\tau'_T$ vs grating period $\Lambda$.

The refractive index change due to increased temperature $\Delta n_T$ is positive whereas the refractive change due to carrier excitation $\Delta n_N$ is negative. The magnitude of these two refractive changes and the corresponding decay times are very different. The result of a numerical calculation of $\Delta n_N$ and $\Delta n_T$ and the total refractive index change $\Delta n$ is shown in Fig. 8. The calculations are based on Eqs. (3) and (14) and have been done for an excitation energy density of $E'=200$ mJ/cm$^2$, a free-carrier grating decay time $\tau/\tau_p=3.4$, and a temperature grating decay time $\tau_T/\tau_p=33$. The temperature coefficient of the refractive index was taken to $\partial n/\partial T=2\times10^{-4}$ K$^{-1}$. In addition, the carrier-density-dependent sample transmission was considered, which explains the different heights of the three main maxima. The calculated time dependence of the diffracted intensity (Fig. 8) is in qualitative agreement with the experimental observations in Figs. 2 and 7. A detailed fit of the calculations to the experiments has not been done because several parameters would have to be adjusted, requiring a larger computing effort.

A simple proof of the thermal mechanism leading to the broad maximum in Fig. 7 was obtained by measuring the half-value period $\tau'_T$ of the decay of maximum for different grating spacings (Fig. 9). The decay time of the thermal grating is obtained from Eq. (11),

$$\tau_T=1.4\tau'_T=\frac{\Lambda^2}{4\pi^2 D_T} \quad . \tag{15}$$

A fit of Eq. (15) to the experimental data in Fig. 9 results in $D_T=0.9\pm0.1$ cm$^2$/s, which is close to the value calculated from the known heat conductivity, density, and specific heat of silicon.[16,33]

## VII. SUMMARY

Light diffracted from a laser-induced grating in silicon exhibits a strongly oscillating time dependence at high excitation energies. The gratings are due to electronic and thermal refractive-index changes with an amplitude large enough to modulate the diffraction efficiency over several maxima of the Bessel function which is characteristic for a thin phase grating. The opposite sign of the electronic and thermal index changes gives rise to an additional maximum in the time dependence of the diffracted light. The decay of the refractive-index grating is characterized by three parameters which correspond to the ambipolar diffusion coefficient of electron-hole pairs, the Auger-recombination coefficient, and the heat diffusivity. These three parameters have been derived from the experiments and are shown to be near to known literature values. This indicates that the interpretation of the complicated time dependence of the diffraction efficiency is basically correct.

## ACKNOWLEDGMENTS

This work was supported by the "Deutsche Forschungsgemeinschaft." We thank the IBM Company, Wacker Chemie GmbH, and Dr. Seifert, Institute für Weikstoffe der Elektrotechnik, TU Berlin, for the silicon samples.

*Permanent address: Technical University of Harbin, Physical Department, Peking, Harbin, Heilongjing, People's Republic of China.

[1]J. P. Woerdman and B. Bölger, Phys. Lett. **30A**, 164 (1969).
[2]J. P. Woerdman, Phys. Lett. **32A**, 305 (1979).
[3]J. P. Woerdman, Opt. Commun. **2**, 212 (1970).
[4]J. P. Woerdman, Philips Res. Rep. Suppl. **8**, 7 (1971).
[5]R. K. Jain and M. B. Klein, Appl. Phys. Lett. **35**, 454 (1979).
[6]R. K. Jain, M. B. Klein, and R. C. Lind, Opt. Lett. **4**, 328 (1979).
[7]F. A. Hopf, A. Tomita, and T. Liepmann, Opt. Commun. **37**, 72 (1981).
[8]E. W. Van Stryland, A. L. Smirl, Th.F. Bogess, M. J. Soileau, B. S. Wherett, and F. A. Hopf, *Proceedings of the Third International Conference on Picosecond Phenomena* (Springer, Berlin, 1982), p. 368.
[9]V. L. Vinetskii, N. V. Kukhtarev, S. G. Odulov, and M. S. Soskin, Zh. Tekh. Fiz. **47**, 1270 (1977) [Sov. Phys.—Tech. Phys. **22**, 729 (1977)].
[10]V. L. Vinetskii, T. E. Zaporozhets, N. V. Kukhutarev, A. S. Matriichuk, S. G. Odulov, and M. S. Soskin, Pis'ma Zh. Eksp. Teor. Fiz. **25**, 432 (1977) [JETP Lett. **25**, 404 (1977)].
[11]G. G. MacFarlane, T. P. McLean, J. E. Quarrington, and V. Roberts, Phys. Rev. **111**, 1245 (1958).
[12]E. H. Sin, C. K. Ong, and H. S. Tan, Phys. Status Solidi A **85**, 199 (1984).
[13]S. G. Odulov, I. I. Peshko, M. S. Soskin, and A. I. Khizhujak, Ukr. Fiz. J. **21**, 1869 (1976).
[14]K. Jarasiunas and S. Vaitkus, Phys. Status Solidi A **44**, 793 (1977).
[15]H. J. Eichler and F Massmann, J. Appl. Phys. **53**, 3237 (1982).
[16]E. Gaubas, K. Jarasiunas, and J. Vaitkus, Phys. Status Solidi A **69**, K87 (1982).
[17]J. Vaitkus, E. Gaubas, K. Yarashyunas, and V. Mikhailov, Fiz. Tekh. Poluprovodn. **17**, 1552 (1983) [Sov. Phys.—Semicond. **17**, 989 (1983)].
[18]S. Komuro, Y. Aoyagai, Y. Segawa, S. Namba, A. Masuyama, H. Okamoto, and Y. Hamakawa, Appl. Phys. Lett. **43**, 968 (1983).
[19]D. M. Shemwell and C. D. Cantrell, J. Appl. Phys. **56**, 1309 (1984).
[20]S. Komuro, Y. Aoyagi, Y. Segawa, S. Namba, A. Masuyama, and K. Tanaka, J. Appl. Phys. **56**, 1658 (1984).
[21]H. J. Eichler, P. Günter, and D. W. Pohl, *Laser-Induced Gratings,* Vol. 50 of *Springer Series in Optical Science* (Springer, Berlin, 1986).
[22]H. Bergner, V. Brückner, and M. Supianek, IEEE J. Quantum Electron. **QE-22**, 1306 (1986).
[23]J. Vaitkus, K. Jarasiunas, and E. Gaubas, L. Jonikas, R. Pranaitis, and L. Subacius, IEEE J. Quantum Electron. **QE-22**, 1298 (1986).
[24]M. Born and E. Wolf, *Principles of Optics* (Pergamon, Oxford, 1975).
[25]K. G. Svantesson, J. Phys. D **12**, 425 (1979).
[26]Gho-Zhen Yang and N. Bloembergen, IEEE J. Quantum Electron. **QE-22**, 195 (1986).
[27]H. M. van Driel, Appl. Phys. Lett. **44**, 617 (1984).
[28]J. Dziewior and W. Smid, Appl. Phys. Lett. **31**, 346 (1977).
[29]K. G. Svantesson and N. G. Nilsson, Solid State Electron. **21**, 1603 (1978).
[30]M. G. Grimaldi, P. Baeri, and E. Rimini, Appl. Phys. A **22**, 107 (1984).
[31]J. F. Young and H. M. van Driel, Phys. Rev. B **26**, 2147 (1982).
[32]H. Bergner and V. Brückner, Phys. Status Solidi A **79**, K85 (1983).
[33]H. F. Wolf, *Silicon Semiconductor Data,* Vol. 9 of *International Series of Monographs on Semiconductors,* edited by H. K. Henisch (Pergamon, Oxford, 1976).